JOURNAL OF COMPUTATIONAL PHYSICS **136,** 41–50 (1997)
ARTICLE NO. CP975690

A Switch to Reduce SPH Viscosity

J. P. Morris[1] and J. J. Monaghan[2]

Mathematics Department, Monash University, Clayton, VIC 3168, Australia

Received May 3, 1996; revised March 4, 1997

Smoothed particle hydrodynamics is a Lagrangian particle method for fluid dynamics which simulates shocks by using an artificial viscosity. Unlike Eulerian methods it is not convenient to reduce the effects of viscosity by means of switches based on spatial gradients. In this paper we introduce the idea of time-varying coefficients which fits more naturally with a particle formulation. Each particle has a viscosity parameter which evolves according to a simple source and decay equation. The source causes the parameter to grow when the particle enters a shock and the decay term causes it to decay to a small value beyond the shock. Tests on one-dimensional shocks and a two-dimensional shock–bubble interaction confirm that the method gives good results.

1. INTRODUCTION

In the numerical solution of compressible gas problems using the Eulerian formulation shocks were originally simulated by using an explicit artificial viscosity or by an implicit viscosity resulting from averaging [14]. All these schemes resulted in substantial smearing of shocks and contact discontinuities, together with excessive vorticity decay. The introduction of switches based on spatial derivatives of suitable variables [19, 15, 4] gave much sharper shocks. Combined with Riemann methods with TVD properties (see [18] for examples) these methods give outstanding results for the dynamics of ideal gases. Their only disadvantage is that the methods can be troublesome to implement when the physics is very complicated, and they can lead to subtle errors [13].

Particle methods such as PIC and SPH are always easy to implement even when the physics is complicated. However, at present they treat shocks by the use of an artificial viscosity which results in much greater smearing of shocks and vorticity decay than current Eulerian methods. The switches used for Eulerian schemes do not seem to have any obvious counterpart in Lagrangian particle methods and considerable effort has therefore gone into devising alternative viscosity limiters. The first of these is to only turn the viscosity on when particles are approaching which removes the viscosity for rarefactions. This simple limiter can often be used, but if the fluid has a natural boundary, as is the case in couette flow or an astrophysical accretion disk, it gives an artificial edge pressure. Other limiters include using the ratio of the divergence and the curl of the velocity field [1] to reduce the viscosity when the magnitude of the vorticity is much greater than that of the divergence.

In this paper we consider an entirely different viscosity limiter. We give each particle a viscosity parameter which evolves according to a simple source and decay equation. The source causes the parameter to grow when the particle enters a shock and the decay term causes it to decay to a small value beyond the shock.

2. THE SPH EQUATIONS

The SPH equations are derived from the continuum equations using an interpolation procedure for disordered points (for a review see [7]). These points have the properties of particles, each of which carries mass m moves with velocity $\mathbf{v}$ and has position $\mathbf{r}$. The equations of motion then determine the acceleration, the thermal energy, and the density at each particle. We only need to consider the acceleration equation which, for particle a has the form

$$\frac{d\mathbf{v}_a}{dt} = -\sum_b m_b \left(\frac{P_a}{\rho_a^2} + \frac{P_b}{\rho_b^2} + \Pi_{ab} \right) \nabla_a W_{ab}, \qquad (1)$$

where the summation is over all particles other than particle a (although in practice only near neighbors contribute), P is the pressure, and ρ is the density. Π_{ab} produces a shear and bulk viscosity, W_{ab} is the interpolating kernel, and ∇_a denotes the gradient of the kernel taken with respect to the coordinates of particle a. The kernel is a function of $|\mathbf{r}_a - \mathbf{r}_b|$ so that its gradient can be written

$$\nabla_a W_{ab} = \mathbf{r}_{ab} F_{ab}, \qquad (2)$$

[1] Current address: School of Civil Engineering, Purdue University, West Lafayette, IN 47907. E-mail: jpmorris@ecn.purdue.edu.
[2] E-mail: jjm@sapphire.maths.monash.e.

0021-9991/97 $25.00

where F_{ab} is a negative scalar function which is symmetric in a and b and $\mathbf{r}_{ab} = \mathbf{r}_a - \mathbf{r}_b$ (this notation for vectors is used throughout this paper). The forces between particles are therefore along the line of centres and both linear and angular momentum are conserved. We use spline-based kernels [7] which are zero when the particle separation is greater than $2h$.

The usual form of Π_{ab} is given by the rule

$$\Pi_{ab} = \begin{cases} -\dfrac{\alpha h \mathbf{v}_{ab} \cdot \mathbf{r}_{ab}}{\bar{\rho}_{ab} |\mathbf{r}_{ab}|^2} \left(\bar{c}_{ab} - 2 \dfrac{h \mathbf{v}_{ab} \cdot \mathbf{r}_{ab}}{|\mathbf{r}_{ab}|^2} \right), & \text{if } \mathbf{v}_{ab} \cdot \mathbf{r}_{ab} < 0, \\ 0, & \text{otherwise,} \end{cases} \tag{3}$$

where α is a nondimensional viscosity parameter, c is the speed of sound, $\bar{c}_{ab} = \frac{1}{2}(c_a + c_b)$, and $\bar{\rho}_{ab} = \frac{1}{2}(\rho_a + \rho_b)$. To prevent a possible singularity when particles meet, the term $|\mathbf{r}_{ab}|^2$ is replaced by $(|\mathbf{r}_{ab}|^2 + \eta^2)$, where $\eta \ll h$.

This viscosity term was constructed in the following way. The term involving the speed of sound was based on the viscosity of a gas. The term involving $(\mathbf{v}_{ab} \cdot \mathbf{r}_{ab})^2$ was constructed to prevent penetration in high Mach number collisions by producing an artificial pressure roughly proportional to ρv^2. The viscosity vanishes for rigid rotation and is galilean invariant.

If the continuum limit of the equations is taken (by taking the limit as the number of particles goes to infinity) the artificial viscosity is found to give a shear and bulk viscosity [12, 6]. For example, the term with the speed of sound produces a shear viscosity coefficient of $ahc/8$ for two-dimensional motion and this is confirmed by numerical experiments [5, 10]. The typical Reynolds number is therefore $8\,VL/(ach)$, where V is a typical velocity varying on a length scale L. Since medium to strong shocks require $\alpha = 1$ and typical resolutions result in $L \sim 25h$, the Reynolds number is $\sim$200 for Mach numbers $\sim$1. This value is acceptable for many simulations but for low Mach number flow the fluid becomes too viscous and angular momentum and vorticity are transferred unphysically. The limiter due to [1] combats this by multiplying Π_{ab} by $\bar{f}_{ab}$, where

$$f_a = \frac{|\nabla \cdot \mathbf{v}|_a}{|\nabla \cdot \mathbf{v}|_a + |\nabla \times \mathbf{v}|_a + \sigma}. \tag{4}$$

In cosmological simulations this viscosity limiter reduces the unphysical spread of angular momentum in galactic disks by a factor of 20 [17]. It has no effect on one-dimensional or planar shocks, although it improves results for shocks hitting density discontinuities obliquely.

3. THE NEW APPROACH

We give each particle its own viscosity parameter α. This parameter is then assumed to evolve according to the equation

$$\frac{d\alpha}{dt} = -\frac{\alpha - \alpha^\star}{\tau} + S. \tag{5}$$

The first term on the right-hand side of Eq. (5) causes α to decay to $\alpha^\star$ with e-folding time τ. We assume here that $\alpha^\star = 0.1$, since this gives an order of magnitude reduction in viscous effects while maintaining order amongst the particles away from shocks. The second term S is a source which causes α to grow as the particle approaches a shock.

There are many possibilities for the choice of τ and S. The time scale really should be chosen according to the postshock states, including the postshock velocity relative to the shock front. Without knowing the structure of the shock we cannot estimate this accurately. As a compromise we use

$$\tau = h/\mathscr{C}_1 c, \tag{6}$$

where $\mathscr{C}_1$ is a nondimensional parameter. This time scale is related to that used by many SPH codes to choose a suitable time step according to the CFL condition. This choice of τ is approximately the time information takes to propagate through a resolution length(h).

A suitable value for $\mathscr{C}_1$ can be determined by the following argument. Consider Eq. (5) just behind a shock, where $S \approx 0$ and α is a maximum:

$$\frac{d\alpha}{dt} = -(\alpha - \alpha^\star)\mathscr{C}_1 \frac{c}{h}. \tag{7}$$

This has the solution,

$$\alpha = \alpha^\star + A \exp(-t/\tau), \tag{8}$$

which describes the exponential decay of viscosity behind the shock. Typically, we want the viscosity to persist for several smoothing lengths behind the shock. The postshock velocity (relative to the shock front) is $M_2 c$, where M_2 is the postshock Mach number. If we equate the time taken to travel $h\delta$ (relative to the shock front) downstream to the e-fold time, we obtain

$$\mathscr{C}_1 = M_2/\delta. \tag{9}$$

It can be shown that the postshock Mach number for strong shocks is

$$M_2 = \sqrt{(\gamma - 1)/2\gamma}, \tag{10}$$

so

$$\mathscr{C}_1 = \frac{1}{\delta}\sqrt{(\gamma - 1)/2\gamma}, \tag{11}$$

For $\gamma = \frac{5}{3}$ we find $\mathscr{C}_1 \approx 0.447/\delta$. Thus, if we wish the viscosity to decay over 2 to 5 smoothing lengths, we have,

$$0.1 < \mathscr{C}_1 < 0.2. \tag{12}$$

In the calculations described later we choose $\mathscr{C}_1 = 0.2$.

We choose S to be

$$S = \max(-\nabla \cdot \mathbf{v}, 0), \tag{13}$$

since this becomes large near shocks and is galilean invariant. Other forms of S are discussed in Section 5.

We can determine the typical peak values of α by considering a particle approaching a shock in one dimension. If we assume that the time taken passing through the shock front (where the source term is largest) is short compared to τ, the decay term can be neglected. We assume that the shock profile is steady at $x = 0$, the fluid velocity is in the negative direction and decreases in magnitude monotonically as fluid passes through the shock front ($\partial v/\partial x < 0$). A frame where the shock front is stationary is chosen to simplify the analysis, but the result remains galilean invariant. In this case, the comoving derivative is

$$\frac{d}{dt} = v(x)\frac{\partial}{\partial x}. \tag{14}$$

Neglecting the decay term, the equation for $\alpha(x)$ becomes

$$v\frac{\partial \alpha}{\partial x} = -\frac{\partial v}{\partial x} \tag{15}$$

for our choice of source term. Thus,

$$\alpha(x) - \alpha^\star = \int_{x'=+\infty}^{x} -\frac{1}{v}\frac{\partial v}{\partial x'}\,dx' \tag{16}$$

$$= -\ln\frac{v}{v_1}, \tag{17}$$

where

$$\lim_{x\to+\infty} v(x) = v_1. \tag{18}$$

Downstream of the shock front,

$$\alpha = \alpha^\star + \ln\frac{v_1}{v_2}, \tag{19}$$

where v_2 is the postshock velocity *relative* to the shock front. For a shock of infinite Mach number in an ideal gas, we have

$$v_2 = \frac{\gamma - 1}{\gamma + 1}v_1 \tag{20}$$

and

$$\alpha = \alpha^\star + \ln\frac{\gamma + 1}{\gamma - 1}. \tag{21}$$

Our one-dimensional tests used an ideal, monatomic equation of state, leading to $\alpha - \alpha^\star$ having a theoretical peak of ~1.39 in the absence of the decay term. The presence of the decay term leads to this peak not being realised. In practice, α was observed to peak at ~1, which is known from many experiments to be a good choice for shocks. Since the peak value of α depends upon the equation of state (γ in Eq. (21)), in general, S should be multiplied by a factor for different choices of γ. For example, our calculations simulating a shock striking a bubble of gas (see Section 4.4) used $\gamma = 1.4$, giving a theoretical peak of ~1.79. The source term was multiplied by $1.39/1.79 \approx 0.77$ to reduce the peak to approximately 1 for strong shocks.

It is also informative to consider the case of a homologous flow,

$$\mathbf{v} = -A\mathbf{r}. \tag{22}$$

In astrophysical problems involving gravitational collapse, the flow may approximate this ideal in some regions and it is important that α remain suitably small in the absence of shocks. This flow gives a constant source term,

$$-\nabla \cdot \mathbf{v} = 3A. \tag{23}$$

Substituting this into Eq. (5) and considering the steady state, we find

$$\alpha = \alpha^\star + 3A\tau \tag{24}$$

$$= \alpha^\star + \frac{3Ah}{\mathscr{C}_1 c}. \tag{25}$$

We see that for rapidly contracting (large A) systems, α could become quite large. As the system contracts, however, h should decrease and c increase, leading to a decrease in α. In practice, an acceptable maximum α for the unshocked fluid should be chosen and Eq. (25) solved to determine an appropriate resolution (h). For some collapse problems, this resolution may be too computationally expensive. Similar analysis could be carried out for alternate source terms which may perform better in such circumstances.

In the numerical calculations which follow, the α we use is the average $0.5(\alpha_a + \alpha_b)$, where a and b are the labels of the two particles. This preserves the symmetry required for the conservation of momentum. The velocity divergence for any particle a is given by

$$\nabla \cdot \mathbf{v} = \frac{1}{\rho_a} \sum_b m_b \mathbf{v}_{ab} \cdot \nabla_a W_{ab}. \tag{26}$$

4. TEST CASES

The simulations presented in the following sections use $\mathscr{C}_1 = 0.2$. The exact choice is not critical, but this value provides good results for a wide range of problems.

4.1. *Stationary Shock Front*

The simplest test case to consider is that of a one-dimensional shock. We will consider the problem in the frame of reference of the shock front. The upstream particle spacing is 1 unit and the smoothing length is 1.2 units. Constant smoothing length was used. The gas was taken to be ideal with $\gamma = \frac{5}{3}$. For strong shocks, therefore, the particle spacing downstream of the shock is about 0.25 units. Figure 1 shows the results of one-dimensional SPH simulations of shocks with Mach number 10 on the left and Mach number 100 on the right. These plots show a close up view of the particle quantities about the shock front which is spread over about three smoothing lengths. Each column of frames displays the velocity, source term, and α. We see that the source term peaks midway in the slope of the shock front, as expected. The shock front is initially centered on $x = 0$. The drift away from $x = 0$ of the shock front in the SPH simulation corresponds to an error of less than one percent in the shock speed. The α viscosity peaks as the particles reach their maximum velocity and decays over several smoothing lengths. When the Mach number is increased by a factor of 10 the peak in the source term increases by a factor of 10 also. However, particles are travelling at 10 times the speed they were in the weaker shock simulation and, thus, spend a tenth of the time passing through the shock front. This leads to α having practically the same maximum value in both simulations. Furthermore, since the e-folding time is similar to a time-step condition, it scales appropriately with the Mach number. There are some small oscillations downstream of the shock which are typical of standard SPH simulations of this kind and are consistent with the accuracy of the method. These oscillations could be removed almost entirely by adjusting C_1 and C_2 to give a higher peak in α or a broader tail region. However, for our purposes, these oscillations were regarded as acceptable.

4.2. *Cold Streams Colliding*

An extreme test case, involving shocks, is that of two cool streams of gas colliding head-on. Since the streams are initially cold, the speed of sound is very low (0.01 in the coordinates used in this simulation) and the Mach number is very high. Again we used an ideal gas with $\gamma = \frac{5}{3}$. The particle spacing in the cold gas is 1 unit with a smoothing length of 1.2 units. Results obtained using SPH with the new viscosity are displayed in Fig. 2. The case on the left involves $M_1 = 10^3$ shock, while that on the right is $M_1 = 10^5$. We see, as before, that the source term peaks strongly at the shock fronts, feeding the viscosity, which then decays rapidly in the wake of the shocks. Although the source term has a much higher peak for the $M_1 = 10^5$ case, the maximum value of α is practically the same. Again, there are slight oscillations behind the shock, which are consistent with the accuracy of the method. We see that the same choice of parameters used for the previous test has led to appropriate behavior in α for a wide range of Mach numbers.

4.3. *One-Dimensional Shock Tube*

For the shock tube problem we consider the same initial conditions used in [16]:

$$\begin{aligned} x < 0.5: &\quad \rho = 1, &\quad p = 1, \\ x > 0.5: &\quad \rho = 0.125, &\quad p = 0.1, \end{aligned} \tag{27}$$

for an ideal gas with $\gamma = 1.4$. A similar shock tube problem was considered in [8] in order to test different formulations of artificial viscosity for use with SPH.

For the SPH simulation N particles were distributed uniformly from 0.5 to 1 and $8N$ in the region 0 to 0.5. The smoothing length h was adjusted throughout the simulation to maintain the number of nearest neighbors constant at about 5. Since the peak value of α is expected to be higher for $\gamma = 1.4$, the source term was multiplied by a factor of ~ 0.77 (as suggested in Section 3) for this test. Equation (11) suggests that $\mathscr{C}_1$ should be changed also. However, the correction is so small that $\mathscr{C}_1 = 0.2$ was used as before. At time $t = 0$ the artificial viscosity is set to one in a small region (several smoothing lengths) about the interface, to allow the shock to develop in the presence of the artificial viscosity. This was done to avoid the relatively large oscilla-

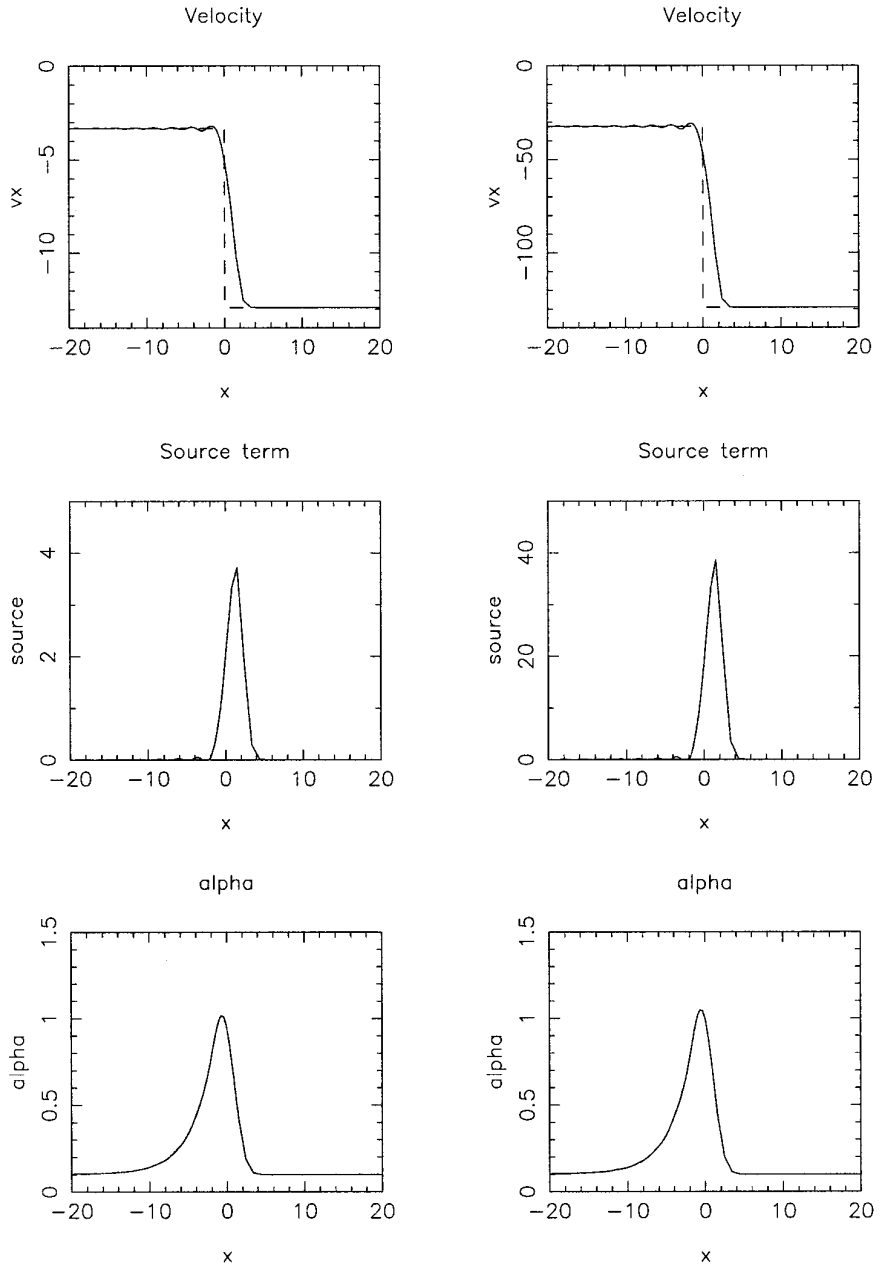

FIG. 1. Results of one-dimensional SPH simulations of a stationary shock with $M_1 = 10$ and $M = 100$. The solid line is the SPH solution and the dashed line is the exact solution. The shock is initially centered on $x = 0$. The drift in shock front position corresponds to an error of less than 1% in the shock speed. The source term is only significant about the shock front. The viscosity tails off rapidly in the wake of the shock after peaking at approximately one for both Mach numbers.

tions that can develop before the source term has had time to increase the artificial viscosity. After this initialisation, the equation for α automatically introduces the necessary viscosity as the shock front propagates.

Figure 3 shows a comparison between the exact results (the dashed line) and the results obtained with SPH using the new approach (isolated points). The shock which develops in this problem is relatively weak, with a mach number of approximately 1.66. Consequently, the peak in the artificial viscosity is reduced to approximately 0.5. The SPH results are in close agreement with the exact results. There are some small postshock oscillations which, if desired, could be removed almost entirely by adjusting C_1 and C_2 (as pointed out previously). There is also a small ''glitch'' in the pressure at the contact discontinuity. This is the result of the jump in internal energy at this interface being

smoothed by the SPH interpolation and thus the SPH pressure is not exactly constant through the interface. It is possible to use alternative expressions for the pressure gradient which do not exhibit this artifact [8]; however, the "glitch" has negligible effect on the fluid motion. The bump in velocity just right of the expansion fan appears to result from slight errors in the initial interpolation at the fluid interface. Increased smoothing of the initial conditions reduces the magnitude of this perturbation.

4.4 *Shock Striking a Bubble*

The tests presented so far are one-dimensional and do not test the method's ability to model flows involving vorticity. In this section we present simulations of a shock striking a bubble of gas for which there are experimental results [3]. This problem has been solved numerically by many authors (for example, [11, 2]) because it is a good test of a numerical method's ability to model shocks, contact

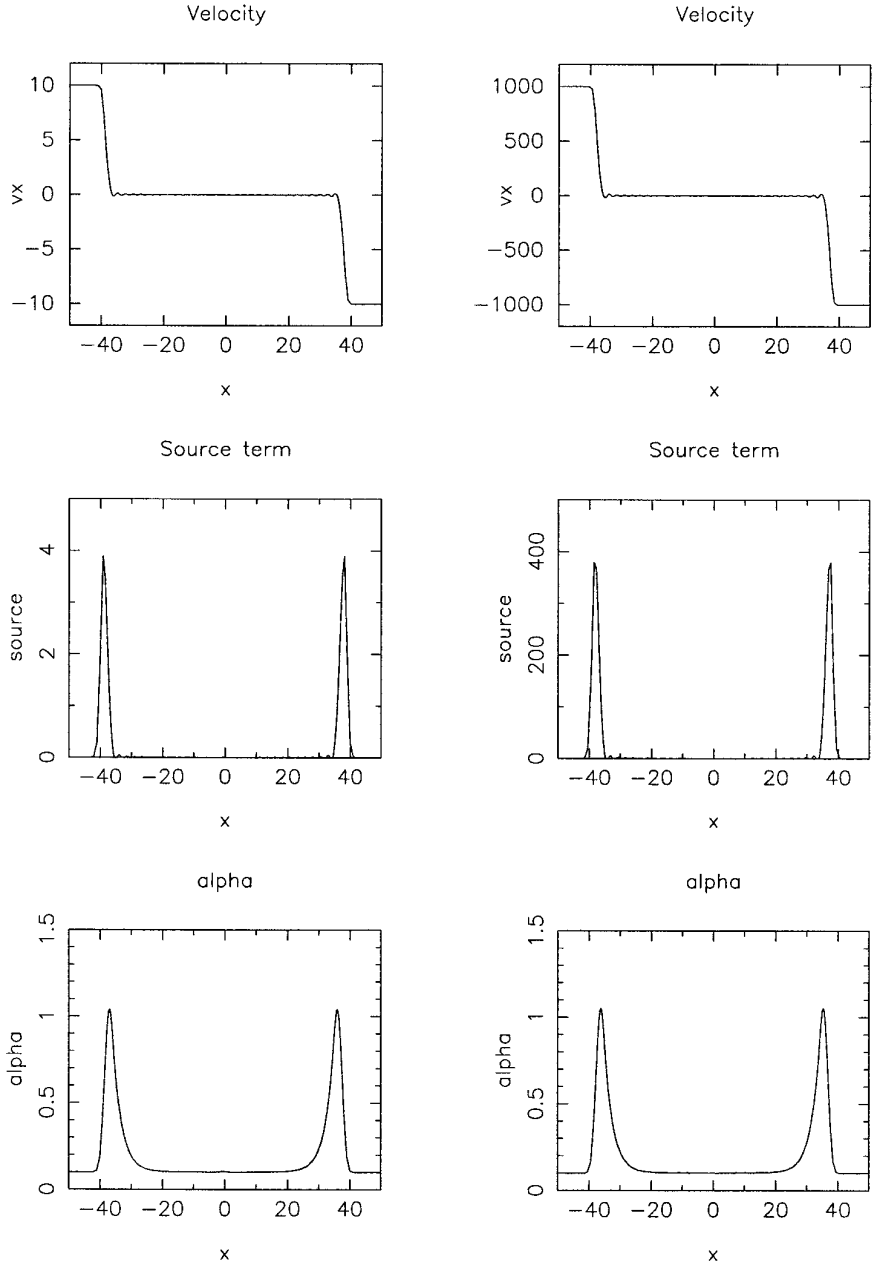

FIG. 2. One-dimensional SPH simulations of cold streams colliding with $M_1 = 10^3$. SPH simulations of cold streams colliding with $M_1 = 10^5$. The source term is only significant about the shock fronts. The viscosity tails off rapidly in the wake of the shocks.

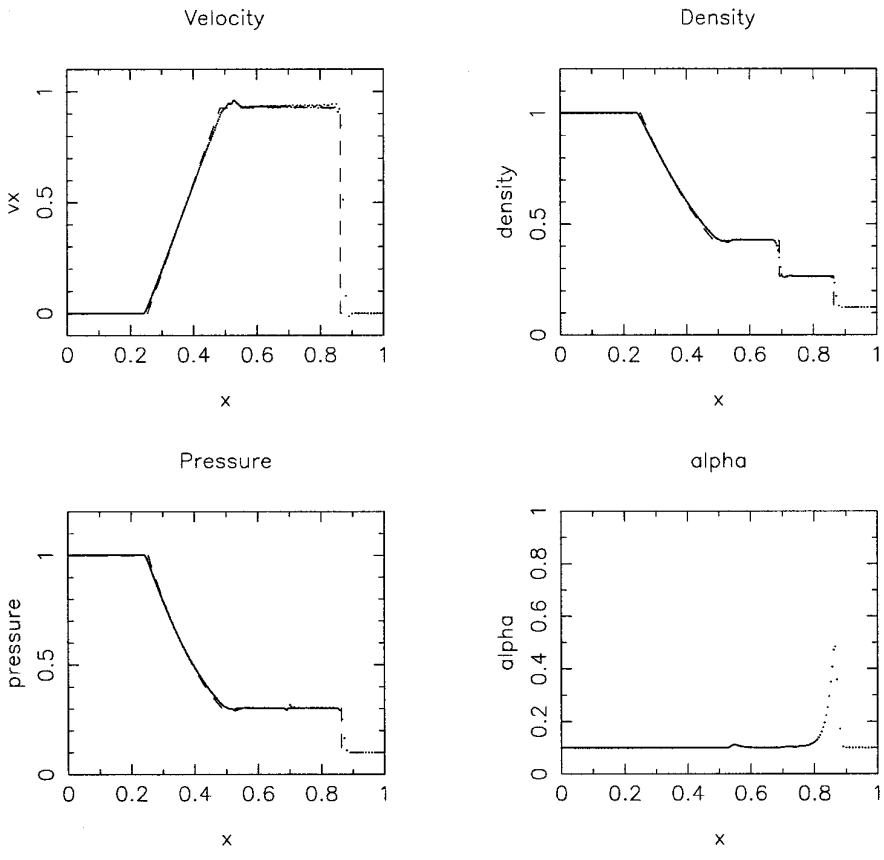

FIG. 3. An SPH simulation of the one-dimensional shock tube problem of [16] using the new method. The dashed line and isolated points represent the exact and SPH solution, respectively (see text for details).

discontinuities, and vorticity generation. The configuration of the shock tube appears in Fig. 4. Here we will only consider results obtained for the case of a weak shock (Mach number 1.23) striking a dense bubble of gas. The shock tube has a diameter of 8.9 cm and the cylinder of gas has a density of 4.64 kg/m^3 and radius 2.5 cm. The surrounding gas has a density of 1.29 kg/m^3.

Typically in standard SPH simulations α is taken to be quite large (often 1) globally. This is necessary, since the viscosity must be present if strong shocks might occur. The present simulation does not involve particularly strong shocks and quite reasonable results may be obtained by taking $\alpha = 0.1$. However, this choice of α presumes prior knowledge of the details of the calculation, whereas general applications involve both strong and weak shocks. We shall, therefore compare results with those obtained using a standard SPH viscosity with $\alpha = 1$.

The results shown here are for an ideal gas with $\gamma = 1.4$ (as did [11]). As in Section 4.3 the source term was multiplied by a factor of $\sim$0.77 and $\mathscr{C}_1$ was chosen to be 0.2. Reflecting boundary conditions were used to model the top half of the tube. The particles all have the same mass and are more densely packed within the cylinder of gas. The initial particle spacing (outside the dense cylinder of gas) was 0.01, the half-width of the tube. The smoothing length varies in space and time such that it is typically 1.2 times the particle spacing. The half-width of the shock tube is therefore approximately 83 resolution lengths. Time integration was carried out using an improved Euler integrator (second-order accurate in time). In order to improve the calculation of pressure gradients at the contact discontinuity, gauge pressure (P_g) was used in the momentum equation (Eq. 1);

$$P_g = P - P_0, \tag{28}$$

where P_0 is the atmospheric pressure. It can be shown [9] that errors in the SPH estimate of the pressure gradient at a contact discontinuity are reduced by this approach, leading to better results for this problem. Momentum is still conserved exactly; however, total energy is approximately conserved.

For comparison, simulations were also carried out using PPM. These employed 100 cells vertically across the top half of the tube. PPM is specifically designed to model shocks and the very fine structures which can form behind

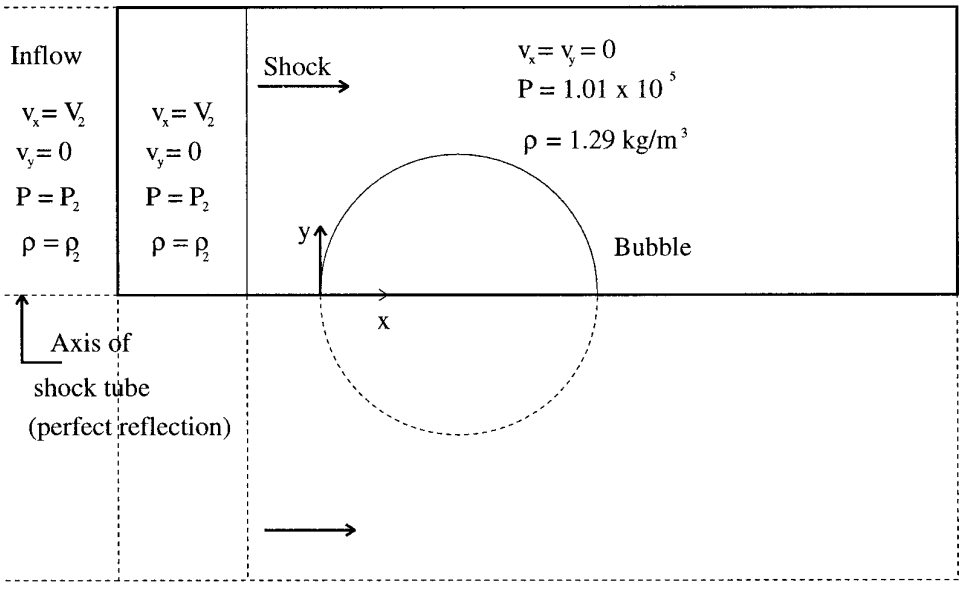

FIG. 4. The shock tube configuration used by [3] in their experiments.

them. It was found that if the bubble interface was not smoothed over a substantial distance, Kelvin–Helmholtz instabilities would develop along the interface in the wake of the shock. For this test, we were most concerned with the formation of vorticity as the shock passes through the bubble and not with the development of smaller scale Kelvin–Helmholtz instabilities. To this end, the initial interface of the cylinder of dense gas was smoothed over 0.4 cm.

Plots of density and vorticity are presented. Since PPM is a cell-based code, it is easy to present results by shading each cell according to the magnitude of the quantity under consideration. The SPH results presented use a similar approach. Centered on the position of each particle a square of size proportional to the smoothing length is drawn in a shade of gray according to the magnitude of the quantity being plotted. Vorticity may be evaluated by SPH using

$$(\nabla \times \mathbf{v})_a = \frac{1}{\rho_a} \sum_b m_b \mathbf{v}_{ab} \times \nabla_a W_{ab}. \tag{29}$$

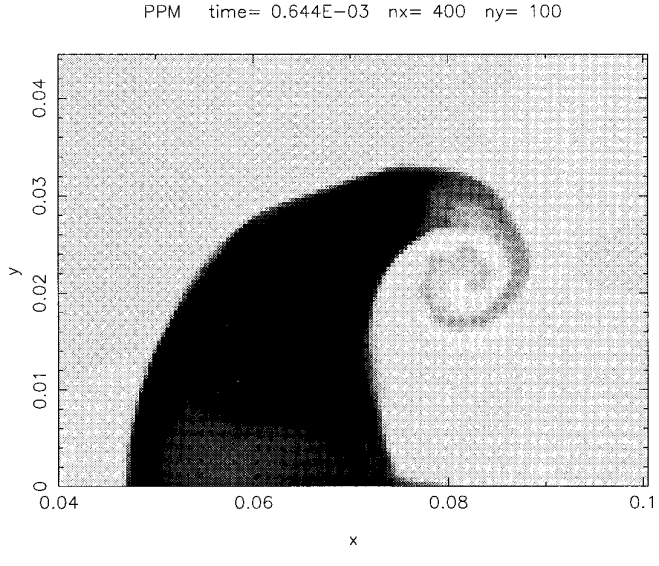

FIG. 5. Result obtained by [9] at $t = 644\ \mu S$ using PPM. The image is shaded from white (1.35 kg/m^3) to black (6 kg/m^3) (see text for details).

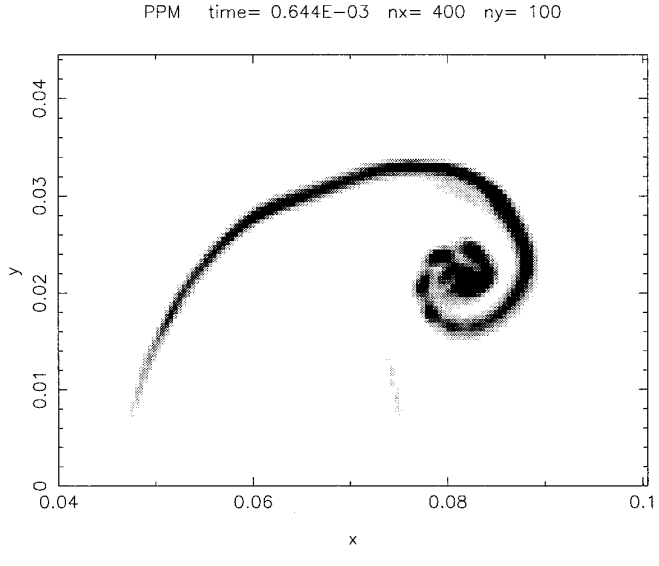

FIG. 6. Vorticity obtained by [9] at $t = 644\ \mu S$ using PPM. The image is shaded from black (-5×10^4 s^{-1}) (see text for details).

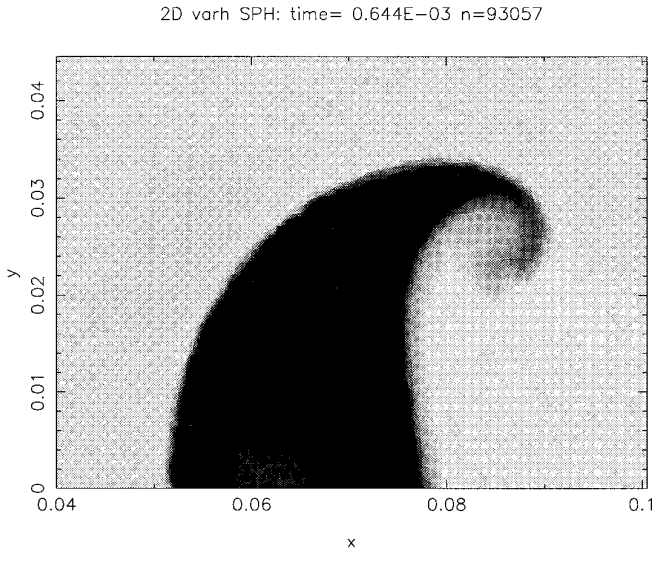

FIG. 7. Result obtained using the standard SPH method ($\alpha = 1$) at $t = 644\ \mu S$. The image is shaded from white (1.35 kg/m^3) to black (6 kg/m^3). The curling up of the bubble in the wake of the shock is inhibited by the large viscosity (see text for details).

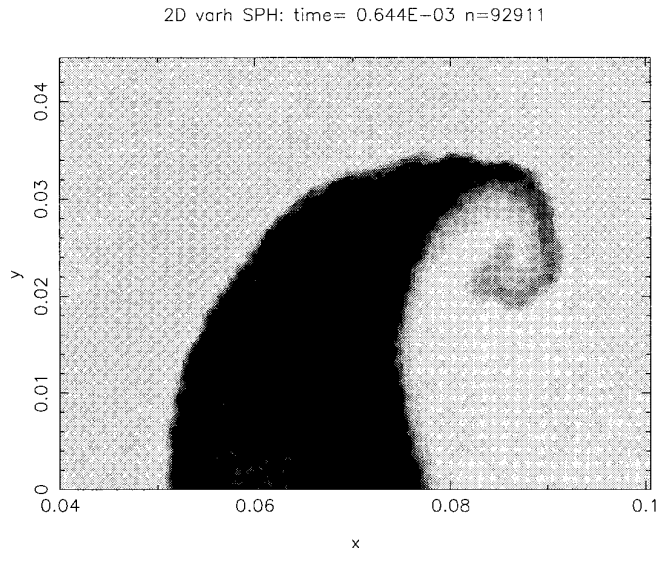

FIG. 9. Results obtained by SPH with the new approach to evolving α at $t = 644\ \mu S$ The image is shaded from white (1.35 kg/m^3) to black (6 kg/m^3) (see text for details).

For the purposes of plotting this quantity, the smoothing lengths were doubled to reduce noise in the results.

The density obtained using the new method (Fig. 9) is a marked improvement over that obtained using the old formulation (Fig. 7) and is in closer agreement with those obtained using PPM (Fig. 5). The simulations do not agree perfectly in their description of the curling up of the bubble. However, the new approach reduces the viscosity so that the vorticity persists, resulting in the curling up of the bubble being further evolved. This is most clear when the vorticity obtained with the new method (see Fig. 10) is compared with that obtained using the old formulation (Fig. 8). The new result has a more extensive region of high vorticity more closely matching that obtained with PPM (Fig. 6). Since a very similar choice of parameters was used as for the previous one-dimensional tests, this approach to evolving the artificial viscosity is very flexible.

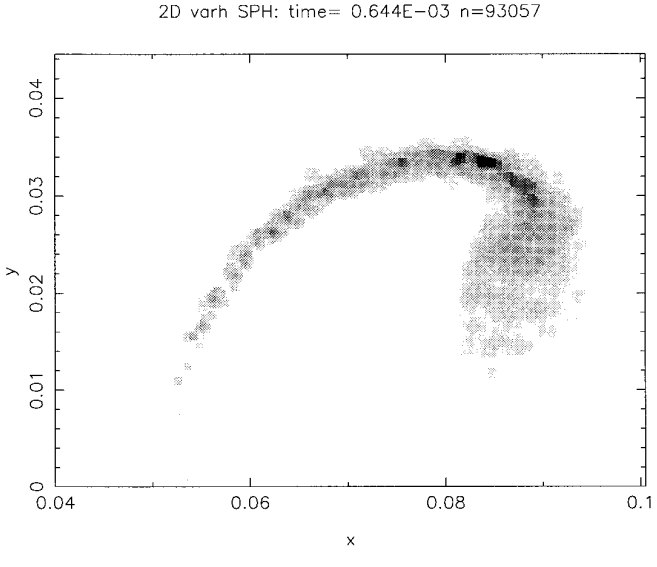

FIG. 8. Vorticity obtained using the standard SPH method ($\alpha = 1$) at $t = 644\ \mu S$. The image is shaded from black (-5×10^4 s^{-1}) to white (-1×10^4 s^{-1}) (see text for details).

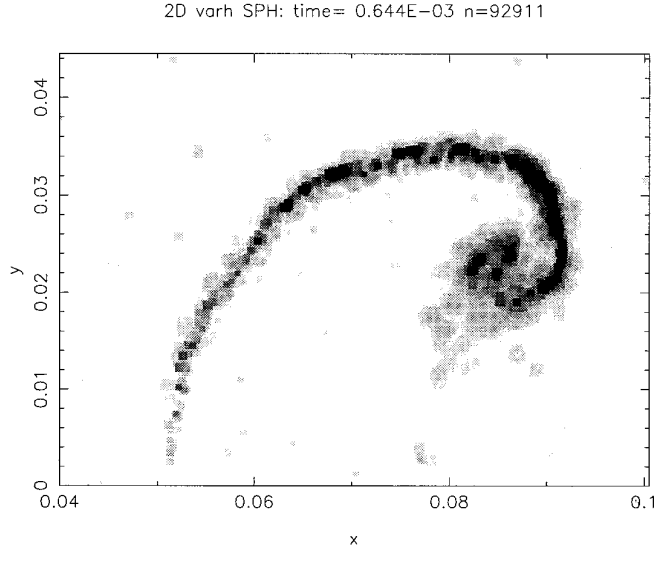

FIG. 10. Vorticity obtained by SPH with the new approach to evolving α at $t = 644\ \mu S$ The image is shaded from black (-5×10^4 s^{-1}) to white (-1×10^4 s$^{-1)}$ to white (-1×10^4 s^{-1}) (see text for details).

5. DISCUSSION AND SUMMARY

We have presented a new approach to the artificial viscosity used by SPH, by allowing the coefficient of viscosity to vary with time. The time variation is determined by an equation with a source term which introduces viscosity on a shock front, and a decay term which rapidly reduces the viscosity behind the shock. This method is very easy to implement and requires little extra memory or time to evaluate. Since the new method reduces the viscosity in regions where it is not needed, lower resolution may be employed to model a given flow, with substantial saving in computer time. For the source and decay terms investigated here, the method appears to be very robust and readily applied to a wide range of problems.

One particular choice of source term was considered in this paper; however there are many possible forms. For example, a source term of the form,

$$S_a = f_a \max(-(\nabla \cdot \mathbf{v})_a, 0) \tag{30}$$

(where f_a is defined by Eq. (4)) may be even more effective at introducing viscosity only where needed. For one-dimensional shocks, this term reduces to the one used in this study; however, when vorticity is present, the source term will be reduced.

Further improvements may be attained by modifying the time scale τ. The choice of τ used in this study resembled the time step required by the CFL condition. It is possible that time scales based on other methods for choosing suitable time integrator steps may provide better performance for some applications.

For the source and decay terms investigated, we have presented an analysis suggesting suitable factors by which the terms should be multiplied. It appears that, for the cases investigated here, source and decay terms should be multiplied by factors which depend upon the equation of state. Once chosen, however, the same coefficients appear to be appropriate to a wide range of problems.

ACKNOWLEDGMENT

The authors thank Tomasz Plewa for allowing us to modify his PPM code to model the interaction of a weak shock and a bubble of gas for comparison with the SPH results.

REFERENCES

1. D. S. Balsara. *J. Comput. Phys.* **121,** 357 (1995).
2. W. S. Don and C. B. Quillen, Numerical simulation of shock-cylinder interactions, *J. Comput. Phys.* **122,** 244 (1995).
3. J.-F.L. Haas and B. Sturtevant, Interaction of weak shock waves with cylindrical and spherical gas inhomogeneities, *J. Fluid Mech.* **181,** 41 (1987).
4. A. Harten, P. D. Lax, and B van Leer, *SIAM Rev.* **25,** 35 (1983).
5. S. T. Maddison, J. R. Murray, and J. J. Monaghan. SPH simulations of accretion disks and narrow rings, *Pub. Aust. Soc. Astro.* **13,** 66 (1996).
6. Z. Meglicki, D. Wickramasinghe, and G. V. Bicknell, *Mon. Not. R. Astron. Soc.* **264,** 691 (1993).
7. J. J. Monaghan, Smoothed particle hydrodynamics, *Annu. Rev. Astron. Astrophys.* **30,** 543 (1992).
8. J. J. Monaghan and R. A. Gingold, *J. Comput. Phys.* **52,** 374 (1983).
9. J. P. Morris, *Analysis of SPH with Applications,* Ph.D. thesis, Mathematics Dept., Monash Univ., Melbourne, Australia, 1996.
10. J. R. Murray, SPH simulations of tidally unstable accretion discs in cataclysmic variables, *Mon. Not. R. Astron. Soc.* **279,** 402 (1996).
11. J. M. Picone and J. P. Boris, Vorticity generation by shock propagation through bubbles in a gas, *J. Fluid Mech.* **189,** 23 (1988).
12. H. Pongracic, *Numerical Modelling of Large Body Impacts,* Ph.D. thesis, Mathematics Dept., Monash University, Melbourne, Australia, 1988.
13. J. J. Quirk, A contribution to the great riemann solver debate, *Int. J. Numer. Methods Fluids* **18,** 555 (1994).
14. R. D. Richtmyer and K. W. Morton, *Difference Methods for Initial-Value Problems,* Wiley-Interscience, New York, 1967.
15. P. L. Roe, *J. Comput. Phys.* **43,** 357 (1981).
16. G. A. Sod, A survey of several finite difference methods for systems of hyperbolic conservation laws, *J. Comput. Phys.* **27,** 1 (1978).
17. M. Steinmetz, *Mon. Not. R. Astron. Soc.* **278,** 1005 (1996).
18. E. F. Toro, *Phil. Trans. Roy. Soc. London* (*A*) **341,** 499 (1992).
19. B. van Leer, *J. Comput. Phys.* **32,** 101 (1979).